

Simulating Continuous-Time Autoregressive Moving Average Processes Driven By p -Tempered α -Stable Lévy Processes

Till Massing*

August 28, 2024

Abstract

We discuss simulation schemes for continuous-time autoregressive moving average (CARMA) processes driven by tempered stable Lévy noises. CARMA processes are the continuous-time analogue of ARMA processes as well as a generalization of Ornstein-Uhlenbeck processes. However, unlike Ornstein-Uhlenbeck processes with a tempered stable driver (see, e.g., Qu et al. (2021)) exact transition probabilities for higher order CARMA processes are not explicitly given. Therefore, we follow the sample path generation method of Kawai (2017) and approximate the driving tempered stable Lévy process by a truncated series representations. We derive a result of a series representation for p -tempered α -stable distributions extending Rosiński (2007). We prove approximation error bounds and conduct Monte Carlo experiments to illustrate the usefulness of the approach.

Keywords: Tempered stable distributions, CARMA processes, Lévy processes, p -tempering, simulation, series representation

2020 Mathematics Subject Classification: 60E07, 60G10, 60G51, 62M10

1 Introduction

We discuss simulation schemes for continuous-time autoregressive moving average (CARMA) processes driven by tempered α -stable Lévy noises. CARMA processes are the continuous-time analogue of discrete-time ARMA processes and extend the concept of Ornstein-Uhlenbeck (OU) processes. Ornstein-Uhlenbeck processes, also referred to as CAR(1), represent the continuous-time analogue of autoregressive processes with a lag order of 1. They find extensive use in financial literature, see, e.g., Barndorff-Nielsen & Shephard (2001). While originally introduced for Gaussian CARMA processes driven by Brownian motion (Brockwell 1994), CARMA processes have been generalized to be driven by arbitrary Lévy processes (Brockwell 2001). Non-negative Lévy-driven CARMA processes have attracted interest, particularly in the context of modeling stochastic volatility (Brockwell et al. 2011). While non-negative OU processes are often employed for this purpose, CARMA processes with higher lag orders offer a more flexible autocorrelation function.

Simulation of Lévy-driven CARMA processes requires the formulation of both a scheme for simulating trajectories of the background-driving Lévy process (BDLP) and a strategy for subsequently sampling a path of the stationary CARMA process. Our primary interest lies in achieving high-frequency sampling to obtain a quasi-continuous sample path. In Todorov & Tauchen (2006) and Kawai (2017), the authors propose series representations of Lévy processes as fundamental building blocks. Series representations for Lévy processes trace back to Rosiński (2001) and provide a method to sample a path with an arbitrary number of jumps. In Kawai (2017) a simple scheme for sampling CARMA paths is presented which is based on a series representation for the BDLP, an approach that we follow in this paper.

We here focus on the special case of CARMA models based on tempered stable distributions which have a long history throughout probability theory and applications in finance. These distributions emerge through the tempering of the Lévy measure of stable distributions with a suitable tempering function. The concept of tempered stable distributions was first introduced by Koponen (1995), who termed the associated Lévy process a “smoothly truncated Lévy flight”, representing a generalization of Tweedie distributions (Tweedie 1984). Subsequently, tempered stable distributions have been generalized in several

*Faculty of Economics, University of Duisburg-Essen, Universitätsstr. 12, 45117 Essen, Germany.
E-Mail: till.massing@uni-due.de

directions, primarily by expanding the class of admissible tempering functions. The seminal paper Rosiński (2007) presents a general framework for tempered stable distributions and derives a series representation which we here extend. The CGMY distribution (Carr et al. 2002) is a well-known special case of the classical tempered stable distribution that was introduced to model log-returns of stock prices. Tempered stable distributions have frequently been used for financial applications (Kim et al. 2008, Rachev et al. 2011, Fallahgoul & Loeper 2019).

In this paper, we treat so-called p -tempered α -stable distributions, as introduced by Grabchak (2012), where $p > 0$ and $\alpha \in (0, 2)$. The parameter p governs the extent of tempering, while α represents the stability index of the associated stable distribution. This class of distributions contains, e.g., the standard class of Rosiński (2007) for $p = 1$ and the class of Bianchi et al. (2011) for $p = 2$. See also Grabchak (2016) for a survey. p -tempered α -stable distributions are potential tools for various financial applications. For example, Sabino (2022) discussed the pricing of a strip of daily European options in energy or commodity markets and the modeling of future markets. Modeling flight length in mobility models is another domain of application as discussed by Grabchak (2016).

Grabchak (2019) develops a fast and easy-to-use rejection sampling algorithm for p -tempered α -stable distributions. However, there is a limitation that we aim to address in this paper. The rejection algorithm requires $0 < \alpha < p$, which leads to the exclusion of important cases. For example, it does not cover instances where $\alpha \in (1, 2)$ for $p = 1$, which is the standard case presented by Rosiński (2007). Therefore, we opt for a different approach by deriving a series representation for p -tempered α -stable distributions that also allows $\alpha > p$. There are a few other series representations available derived by Rosiński & Sinclair (2010) which we briefly review in Section 2.

As previously mentioned, CARMA processes are a natural extension of OU processes. In the literature, simulation algorithms for tempered stable OU processes have been extensively studied. Notably, there exist two distinct versions of these processes with a subtle yet crucial difference. Firstly, TS-OU processes are OU processes having a tempered stable distribution as stationary marginal distribution. Secondly, OU-TS processes are OU processes driven by a tempered stable BDLP. Both variants have been examined in, among others, Zhang & Zhang (2009), Kawai & Masuda (2011a) and Qu et al. (2021). These studies have derived transition probabilities and exact sampling schemes for tempered stable subordinators. Various extensions have since been established. For instance, Sabino & Petroni (2022) and Grabchak & Sabino (2023) have expanded upon these methodologies to simulate TS-OU and OU-TS processes using classical tempered stable distributions and p -tempered stable distributions, respectively. However, the approach of explicitly deriving the transition probabilities is not transferable to general CARMA processes of higher lag order due to the more complicated structure than OU processes (sum of exponential functions instead of one exponential function), see also Kawai (2017). Furthermore, considering a TS-CARMA process – a CARMA process having a stationary TS distribution – is computationally infeasible. Therefore, we focus on the sampling of CARMA processes driven by a tempered stable Lévy process, called CARMA-TS processes, specifically utilizing p -tempered stable distributions.

The contributions of this paper are the following. Firstly, we establish a novel series representation for p -tempered α -stable distributions by generalizing the findings of Rosiński (2007). Based on this, we then derive a series representation and hence a simulation scheme for CARMA processes driven by p -tempered α -stable Lévy processes and we study approximation errors.

The paper is organized as follows. In Section 2 we define p -tempered stable distributions and highlight some important subclasses. Section 3 presents the basics of CARMA processes and some useful properties. In Section 4.1 we state and prove the main theoretical result of a series representation for p -tempered stable Lévy processes. In Section 4.2 we derive the simulation scheme for CARMA-TS processes. Monte Carlo experiments in Section 5 illustrate the usefulness of the proposed simulation scheme and show its limitations. Section 6 concludes. The proofs are to be found in Appendix A.

2 Tempered stable distributions

In this section, we briefly review tempered stable distributions as in Rosiński (2007). We particularly emphasize the extension of these distributions known as p -tempered stable distributions introduced by Grabchak (2012) and reviewed in Grabchak (2016). At the end of the section, we provide relevant examples. To start, we recall some relevant results from probability theory. An \mathbb{R} -valued process $\{L_t\}_{t \in \mathbb{R}_+}$ is called a *Lévy process* if $X_0 = 0$ a.s., it has independent and stationary increments, it is stochastically continuous and the path function is càdlàg a.s. A *subordinator* is a one-dimensional, (a.s.) non-decreasing Lévy process. We express Lévy process using the Lévy-Khintchine representation, i.e., a probability

distribution μ on \mathbb{R}^d of a random variable X is infinitely divisible if and only if there exists a unique triple (called Lévy triple) (γ, A, M) , where M is a measure on \mathbb{R}^d called *Lévy measure*.

Definition 1. Let $\alpha \in (0, 2)$ and $p > 0$. An infinitely divisible probability measure μ on \mathbb{R}^d is called *p-tempered α -stable distribution* if it has no Gaussian part and its Lévy measure has the form

$$M(A) = \int_{\mathbb{S}^{d-1}} \int_0^\infty \mathbf{1}_A(ru) q(r^p, u) r^{-\alpha-1} dr \sigma(du), \quad A \in \mathcal{B}(\mathbb{R}^d), \quad (1)$$

where σ is a finite Borel measure on \mathbb{S}^{d-1} and $q : (0, \infty) \times \mathbb{S}^{d-1} \rightarrow (0, \infty)$ is a Borel function such that, for all $u \in \mathbb{S}^{d-1}$, $q(\cdot, u)$ is *completely monotone* (see Rosiński (2007)) and is called *tempering function*. If

$$\lim_{r \downarrow 0} q(r, u) = 1, \quad (2)$$

for each $u \in \mathbb{S}^{d-1}$, then μ is called a *proper p-tempered α stable distribution*. We call the class of proper p-tempered α -stable distributions TS_α^p .

The tempering function can be represented as

$$q(r^p, u) = \int_0^\infty e^{-r^p s} Q(ds|u),$$

where $\{Q(\cdot|u)\}_{u \in \mathbb{S}^{d-1}}$ is a measurable family of Borel measures. $Q(\cdot|u)$ is a probability measure if and only if (2) holds, i.e., μ is proper.

Proper p-tempered α -stable distributions μ are infinitely divisible. Hence, they induce Lévy processes $L = \{L_t\}_{t \in \mathbb{R}_+}$ s.t. $L_1 \sim \mu$. We call L a *p-tempered α -stable Lévy process*. In this paper, we focus on CARMA processes driven by proper tempered stable Lévy processes. These particular processes align with the initial motivation by modifying the tails of stable distributions to make them lighter to, e.g., obtain finite moments.

Next, we introduce some further measures on \mathbb{R}^d which are related to the Lévy measure M . They are needed later in the proofs and for the simulation scheme of the series representation. We define the Borel measure

$$Q(A) := \int_{\mathbb{S}^{d-1}} \int_0^\infty \mathbf{1}_A(ru) Q(ds|u) \sigma(du), \quad A \in \mathcal{B}(\mathbb{R}^d).$$

Then $Q(0) = 0$. We also define the Borel measure

$$R(A) := \int_{\mathbb{R}^d} \mathbf{1}_A \left(\frac{v}{\|v\|^{1+1/p}} \right) \|v\|^{\alpha/p} Q(dv), \quad A \in \mathcal{B}(\mathbb{R}^d). \quad (3)$$

Also, $R(0) = 0$. The measure R is called the *Rosiński measure*, see Rosiński (2007). We have the change of variable formula

$$\int_{\mathbb{R}^d} F(w) R(dw) = \int_{\mathbb{R}^d} F \left(\frac{v}{\|v\|^{1+1/p}} \right) \|v\|^{\alpha/p} Q(dv),$$

for any Borel function F in the sense that if and only if one side exists then so does the other and both are equal. There is a one-to-one relationship between the Lévy measure and the Rosiński measure, see (Grabchak 2016).

For $p = 1$ we have the special case of tempered α -stable distributions as discussed in the seminal paper of Rosiński (2007). The p-tempered stable distributions we discuss constitute a specific subset of the generalized tempered stable distributions introduced by Rosiński & Sinclair (2010) but have additional structure and cover various interesting subclasses. Moreover, many theoretical results that are available for tempered stable distributions of Rosiński (2007) have an extended version in Grabchak (2016) while a general result for the generalized class of Rosiński & Sinclair (2010) lacks. In the following subsection, we introduce some one-dimensional examples which can be found in the literature and are used in the Monte Carlo experiment in Section 5.

We briefly review different method of series representations to sample paths of tempered stable distributions. The method we propose in Section 4 for general p is an extension of Rosiński (2007) for $p = 1$. There are a few other well-known representations (inverse Lévy method, rejection method, and thinning method) which are compared in Imai & Kawai (2011), Kawai & Masuda (2011b). The inverse method and the rejection method (as a series representation, not to be confused with the rejection

sampling of Grabchak (2019)) have been extended by Rosiński & Sinclair (2010) for general tempered stable distributions which include TS_α^p . We opt for the aforementioned series representation because the inverse method is numerically more challenging, see Imai & Kawai (2013), and the rejection method may have a high number of rejections if the level of truncation is small, see Section 5 for more details. For further numerical properties of series representations see also Kawai (2021), Yuan & Kawai (2021).

Example 1. The first special case is the p -tempered stable subordinator (pTSS). It is constructed from the stable subordinator which is a non-negative, increasing Lévy process with α -stable marginals. In this case, α needs to be in $(0, 1)$. Its Lévy measure is

$$M(dz) = \frac{e^{-(\lambda z)^p} \delta}{z^{1+\alpha}} \mathbb{1}_{(0, \infty)}(z) dz,$$

where $\delta > 0$ is a scale parameter and $\lambda > 0$ a tempering parameter.

Example 2. One-dimensional classical p -tempered stable (pCTS) distributions are defined by their Lévy measure

$$M(dz) = \left(\frac{e^{-(\lambda_+ z)^p} \delta_+}{z^{1+\alpha}} \mathbb{1}_{(0, \infty)}(z) + \frac{e^{-(\lambda_- |z|)^p} \delta_-}{|z|^{1+\alpha}} \mathbb{1}_{(-\infty, 0)}(z) \right) dz.$$

$\alpha \in (0, 2)$ is the stability parameter, $\delta_+, \delta_- > 0$ are scaling parameters, $\lambda_+, \lambda_- > 0$ are tempering parameters. The indices $+$ and $-$ refer to the positive and negative tails of the distribution.

Example 3. Third, we discuss the gamma p -tempered stable distribution (pΓTS), see Terdik & Woyczynski (2006) and Grabchak (2016). For simplicity, we only consider the subordinator case which is one-sided with $\alpha \in (0, 1)$. The Lévy measure is

$$M(dz) = \left(\frac{z^p}{\lambda} + 1 \right)^{-\beta/p} z^{-1-\alpha} \mathbb{1}_{(0, \infty)}(z) dz,$$

where $\beta > 0, \lambda > 0$ are tempering parameters.

3 CARMA processes

In this section, we briefly collect facts for general CARMA processes from Brockwell (2001), Brockwell et al. (2011), Brockwell (2014).

Let $\mathbf{A} \in \mathbb{R}^{\bar{p} \times \bar{p}}$, $\mathbf{b} \in \mathbb{R}^{\bar{p}}$, $\mathbf{e}_{\bar{p}} \in \mathbb{R}^{\bar{p}}$ be defined by

$$\mathbf{A} := \begin{pmatrix} 0 & 1 & 0 & \cdots & 0 \\ 0 & 0 & 1 & \cdots & 0 \\ \vdots & \vdots & \vdots & \ddots & \vdots \\ -a_{\bar{p}} & -a_{\bar{p}-1} & -a_{\bar{p}-2} & \cdots & -a_1 \end{pmatrix}, \quad \mathbf{a} := \begin{pmatrix} a_1 \\ b_2 \\ \vdots \\ a_{\bar{p}-1} \\ a_{\bar{p}} \end{pmatrix}, \quad \mathbf{b} := \begin{pmatrix} b_0 \\ b_1 \\ \vdots \\ b_{\bar{p}-2} \\ b_{\bar{p}-1} \end{pmatrix}, \quad \mathbf{e}_{\bar{p}} := \begin{pmatrix} 0 \\ 0 \\ \vdots \\ 0 \\ 1 \end{pmatrix},$$

where $a_1, \dots, a_{\bar{p}}, b_0, \dots, b_{\bar{p}-1} \in \mathbb{R}$ such that $b_{\bar{q}} = 1$, $\bar{q} \leq \bar{p} - 1$ and $b_k = 0$ for $k > \bar{q}$. Define the autoregressive and the moving average polynomials by

$$a(z) := z^{\bar{p}} + a_1 z^{\bar{p}-1} + \cdots + a_{\bar{p}}, \quad b(z) := b_0 + b_1 z + \cdots + b_{\bar{q}} z^{\bar{q}}, \quad b_{\bar{q}} = 1.$$

Let $\lambda_1, \dots, \lambda_{\bar{p}}$ be the eigenvalues of \mathbf{A} .

We define a Lévy-driven CARMA(\bar{p}, \bar{q}) process $\{Y_t\}_{t \in \mathbb{R}}$ in \mathbb{R} by

$$Y_t := \mathbf{b}^T \mathbf{X}_t, \tag{4}$$

for $t \in \mathbb{R}$, where $\{\mathbf{X}_t\}_{t \in \mathbb{R}}$ solves

$$\mathbf{X}_t = e^{\mathbf{A}(t-s)} \mathbf{X}_s + \int_s^t e^{\mathbf{A}(t-r)} \mathbf{e}_{\bar{p}} dL_r, \quad s \leq t, \tag{5}$$

where $\{L_t\}_{t \in \mathbb{R}}$ is a one-dimensional two-sided Lévy process defined on \mathbb{R} .

Assumption 1. *The two polynomials $a(z)$ and $b(z)$ have no common roots and all roots of $a(z)$ are real, negative and distinct.*

Under this assumption the Lévy-driven CARMA process $\{Y_t\}_{t \in \mathbb{R}}$ is unique and strictly stationary and can be written as

$$Y_t = \int_{-\infty}^{\infty} g(t-s) dL_s,$$

where the function

$$g(t) = \mathbf{b}^T e^{\mathbf{A}t} \mathbf{e}_{\bar{p}} \mathbf{1}_{[0, \infty)}(t) \quad (6)$$

is known as the *kernel* of $\{Y_t\}$. Moreover, by Brockwell et al. (2011), we have

Lemma 1. *Under Assumption 1, the CARMA(\bar{p}, \bar{q}) process can be written as the sum of \bar{p} dependent and possibly complex-valued CAR(1), i.e., Ornstein-Uhlenbeck (OU) processes. That is,*

$$Y_t = \sum_{k=1}^{\bar{p}} Y_t^{(k)} := \sum_{k=1}^{\bar{p}} \int_{-\infty}^t \alpha_k e^{\lambda_k(t-s)} dL_s,$$

where

$$\alpha_k = \frac{b(\lambda_k)}{a'(\lambda_k)}, \quad k = 1, \dots, \bar{p}, \quad (7)$$

and a' denotes the first derivative of a .

Definition 2. Let $p > 0$, $\alpha \in (0, 2)$. Let $\{L_t\}_{t \in \mathbb{R}}$ be a TS_{α}^p process. Let $\bar{q} \leq \bar{p} - 1$ and let $a(z)$ and $b(z)$ be polynomials such that Assumption 1 is satisfied. We call the process $\{Y_t\}_{t \in \mathbb{R}}$ defined by (4) and (5) CARMA(\bar{p}, \bar{q})- p TS process (or short CARMA- p TS process). For $\bar{p} = 1, \bar{q} = 0$, CAR(1) processes are called OU- p TS processes.

We end the section with a notational remark highlighting the difference between p (the tempering parameter) and \bar{p} (the AR lag order) and the difference between α (the stability index) and the α_k 's from (7).

4 Theoretical results

This section is divided into two subsections. In the first, we prove the main theorem for a series representation for p -tempered stable Lévy distributions. In the second, we discuss resulting algorithms and approximation errors for simulating CARMA- p TS processes.

4.1 Series representation for p -tempered stable distributions

In this subsection we derive a series representation for p -tempered α -stable distributions and Lévy processes. We generalize the results of Rosiński (2007) for tempered stable distributions, i.e., $p = 1$ and Bianchi et al. (2011) for $p = 2$.

Theorem 1. *Let $p > 0$ and $T > 0$. Let $\{E_j\}$ and $\{E'_j\}$ be i.i.d. sequences of standard exponentials. Let $\{T_j\}$ be an i.i.d. sequence of uniforms on $(0, T)$. Let $\{U_j\}$ be an i.i.d. sequence of uniforms on $(0, 1)$. Let $\{V_j\}$ be an i.i.d. sequence of random vectors with distribution $Q/||\sigma||$. We assume all sequences to be independent. Set $\Gamma_j := E'_1 + \dots + E'_j$. $\{\Gamma_j\}$ forms a Poisson point process on $(0, \infty)$ with the Lebesgue intensity measure.*

(i) *If $\alpha \in (0, 1)$, or if $\alpha \in [1, 2)$ and Q is symmetric, define*

$$L_t := \sum_{j=1}^{\infty} \mathbf{1}_{(0, t]}(T_j) \left(\left(\frac{\alpha \Gamma_j}{||\sigma|| T} \right)^{-1/\alpha} \wedge \frac{E_j^{1/p} U_j^{1/\alpha}}{||V_j||^{1/p}} \right) \frac{V_j}{||V_j||}, \quad t \in [0, T]. \quad (8)$$

Then the series (8) converges a.s. uniformly in $t \in [0, T]$ to a Lévy process L such that $L_1 \sim \mu \in TS_{\alpha}^p$ with Lévy measure M as in (1).

(ii) If $\alpha \in [1, 2)$ and if Q is non-symmetric and $1+p \neq \alpha$ and additionally assuming $\int_{\mathbb{R}^d} \|w\| R(dw) < \infty$ for $\alpha \in (1, 2)$ and $\int_{\mathbb{R}^d} \|w\| |\log \|w\|| R(dw) < \infty$ for $\alpha = 1$, define

$$L_t := \sum_{j=1}^{\infty} \mathbf{1}_{(0,t]}(T_j) \left(\left(\frac{\alpha \Gamma_j}{\|\sigma\| T} \right)^{-1/\alpha} \wedge \frac{E_j^{1/p} U_j^{1/\alpha}}{\|V_j\|^{1/p}} \right) \frac{V_j}{\|V_j\|} - \frac{t}{T} \left(\frac{\alpha j}{\|\sigma\| T} \right)^{-1/\alpha} x_0 + tb_T, \quad t \in [0, T], \quad (9)$$

where

$$x_0 = \mathbb{E} \left[\frac{V_j}{\|V_j\|} \right] = \|\sigma\|^{-1} \int_{\mathbb{R}^d} u \sigma(du),$$

and

$$b_T = \begin{cases} \alpha^{-1/\alpha} \zeta\left(\frac{1}{\alpha}\right) (\|\sigma\| T)^{1/\alpha} T^{-1} x_0 + \frac{1}{\alpha-1} \Gamma\left(\frac{1+p-\alpha}{p}\right) x_1, & 1 < \alpha < 2, \\ \left(\frac{\gamma+p}{p} + \log(\|\sigma\| T)\right) x_1 - \int_{\mathbb{R}^d} w \log \|w\| R(dw), & \alpha = 1, \end{cases} \quad (10)$$

where

$$x_1 = \int_{\mathbb{R}^d} w R(dw),$$

and ζ denotes the Riemann zeta function. Then the series (9) converges a.s. uniformly in $t \in [0, T]$ to a Lévy process L such that $L_1 \sim \mu \in TS_{\alpha}^p$ with Lévy measure M as in (1).

For simulation, the infinite series representations (8) and (9) need to be truncated. We follow Imai & Kawai (2011) to derive the truncation error for p -tempered α -stable Lévy processes.

Theorem 2. Let $p > 0$, $\alpha \in (0, 2)$ and $T > 0$. Let L be a p -tempered α -stable Lévy process with Lévy measure M . For $n \in \mathbb{N}$, let

$$L_t^{(n)} := \sum_{\Gamma_j \leq Tn} \mathbf{1}_{(0,t]}(T_j) H(\Gamma_j; (V_j, E_j, U_j)) - \frac{t}{T} \mathbb{E} [H(\Gamma_j; (V_j, E_j, U_j))], \quad t \in [0, T],$$

where $T_j, \Gamma_j, V_j, E_j, U_j$ are as in Theorem 1 and H given in (19). Then, $L^{(n)}$ is a compound Poisson process with characteristic triplet $(0, 0, M_n)$ and converges to the characteristic triplet $(0, 0, M)$ as $n \rightarrow \infty$, where

$$M_n((x, \infty)B) = \left(n \frac{\alpha}{\|\sigma\|} x^{\alpha} \wedge 1 \right) M((x, \infty)B), \quad (11)$$

for $x > 0$ and $B \in \mathcal{B}(\mathbb{S}^{d-1})$.

4.2 CARMA-pTS process

In this subsection, we discuss path simulation of stationary CARMA-pTS processes, i.e., CARMA processes driven by a p -tempered α -stable Lévy process. We follow Kawai (2017) to derive a series representation with the help of Theorem 1. Let $\{Y_t\}_{t \in \mathbb{R}}$ be a CARMA(\bar{p}, \bar{q}) process driven by $\{L_t\}_{t \in \mathbb{R}}$, a one-dimensional p -tempered α -stable Lévy process on the real line. Let $T > 0$. We aim to simulate the path on $[0, T]$. The method of Kawai (2017) is based on the following decomposition

$$Y_t = Y_t(\kappa, n) + Q_t(n) + R_t(\kappa, n),$$

where $\kappa > 0$ and $n \in \mathbb{N}$. n denotes the level of truncation of small jumps as in Theorem 1. κ is the threshold of jump times. $Y_t(\kappa, n)$ is exactly simulatable with a series representation. $Q_t(n)$ are the very small jumps which may be approximated by a Gaussian CARMA process. $R_t(\kappa, n)$ are the jumps which occurred before time $-\kappa$ and are to be discarded (or replaced by their mean). There are two different methods for simulation of CARMA-pTS processes to use depending on whether the tempered stable Lévy process is a subordinator or not. We start with the case when L is not a subordinator.

Let M denote the Lévy measure for a one-dimensional TS_{α}^p process as in (1). Note that $M(\mathbb{R}) = \infty$ and the variance $\int_{\mathbb{R}} z^2 M(dz) < \infty$. Let $\{M_n\}_{n \in \mathbb{N}}$ be a family of measures approximating M such that for each n , $M_n(\mathbb{R}) = n$ and $M_n(A) \leq M(A)$ for $A \in \mathcal{B}(\mathbb{R})$. An example of such a family is the family $\{M_n\}$ of Theorem 2. Define the variance of discarded jumps

$$\sigma_n^2 := \int_{\mathbb{R}} z^2 (M - M_n)(dz). \quad (12)$$

Kawai (2017) showed that, if for each $c > 0$

$$\frac{1}{\sigma_n^2} \int_{\{z^2 > c\sigma_n^2\}} z^2 (M - M_n)(dz) \rightarrow 0 \quad (13)$$

for $n \rightarrow \infty$, then

$$\left\{ \frac{Q_t(n)}{\sigma_n} \right\}_{t \in [0, T]} \xrightarrow{\mathcal{D}} \left\{ \int_{-\infty}^T \int_{\mathbb{R}} g(t-s) dW_s \right\}_{t \in [0, T]},$$

where $\{W_t\}_{t \in [0, T]}$ is a two-sided Brownian motion. Furthermore, it holds that for each $n \in \mathbb{N}$, $\{R_t(\kappa, n)\}_{t \in [0, T]}$ converges in probability to the zero process uniformly on $[0, T]$ as $\kappa \rightarrow \infty$. Section 3.3 of Cohen & Rosiński (2007) shows that (13) holds (for multivariate) tempered α -stable processes. Their result can be easily extended to p -tempered stable processes.

Therefore, together with Theorems 1 and 2 we can propose the following approximation schemes. We stress the difference between the variance of discarded jumps σ_n^2 and $\|\sigma\|$ of the Borel measure σ .

Scheme 1. Let $T > 0, \kappa > 0$. Let $p > 0, \alpha \in (0, 2)$. Let $\{L_t\}_{t \in \mathbb{R}}$ be a $TS_{\alpha}^{\bar{p}}$ process with Lévy measure M . Let $\{W_t\}_{t \in \mathbb{R}}$ be a Brownian motion. Let $\bar{q} \leq \bar{p} - 1$ and let $a(z)$ and $b(z)$ be polynomials such that Assumption 1 is satisfied and α_k and λ_k for $k = 1, \dots, \bar{p}$ as in Lemma 1. Let $\{Y_t\}_{t \in \mathbb{R}}$ be a CARMA- p TS process.

Let $n \in \mathbb{N}$ and σ_n^2 as in (12) and $\sigma_n := \sqrt{\sigma_n^2}$. Let $Z_{\kappa, n}$ be a Poisson random variable with mean $(T + \kappa)n$. Let $\{\Lambda_{(j)}\}_{j=1, \dots, Z_{\kappa, n}}$ be the ascending order statistic of $Z_{\kappa, n}$ i.i.d. uniform random variables on $(0, \alpha n / \|\sigma\|)$. Let $\{E_j\}$ be a i.i.d. sequence of standard exponentials. Let $\{T_j\}$ be an i.i.d. sequence of uniforms on $(-\kappa, T)$. Let $\{U_j\}$ be an i.i.d. sequence of uniforms on $(0, 1)$. Let $\{V_j\}$ be an i.i.d. sequence of random vectors with distribution $Q / \|\sigma\|$. We assume all sequences to be independent.

Then, Y_t for $t \in [0, T]$ can be approximated by

(i) if $\alpha \in (0, 1)$, or if $\alpha \in [1, 2)$ and Q is symmetric,

$$\sum_{k=1}^{\bar{p}} \sum_{j=1}^{Z_{\kappa, n}} \alpha_k e^{\lambda_k(t-T_j)} \mathbb{1}_{(-\kappa, t]}(T_j) \left(\Lambda_{(j)}^{-1/\alpha} \wedge \frac{E_j^{1/p} U_j^{1/\alpha}}{\|V_j\|^{1/p}} \right) \frac{V_j}{\|V_j\|} + \sigma_n \int_{-\infty}^t \alpha_k e^{\lambda_k(t-s)} dW_s \quad (14)$$

(ii) if $\alpha \in [1, 2)$ and if Q is non-symmetric and $1 + p \neq \alpha$, additionally assuming $\int_{\mathbb{R}^d} \|w\| R(dw) < \infty$ for $\alpha \in (1, 2)$ and $\int_{\mathbb{R}^d} \|w\| |\log \|w\|| R(dw) < \infty$ for $\alpha = 1$,

$$\begin{aligned} & \sum_{k=1}^{\bar{p}} \left[\sum_{j=1}^{Z_{\kappa, n}} \alpha_k e^{\lambda_k(t-T_j)} \mathbb{1}_{(-\kappa, t]}(T_j) \left(\Lambda_{(j)}^{-1/\alpha} \wedge \frac{E_j^{1/p} U_j^{1/\alpha}}{\|V_j\|^{1/p}} \right) \frac{V_j}{\|V_j\|} + \alpha_k \frac{1 - e^{\lambda_k(t+\kappa)}}{\lambda_k(T + \kappa)} \left(\frac{\alpha_j}{\|\sigma\|(T + \kappa)} \right)^{-1/\alpha} x_0 \right. \\ & \left. - \alpha_k \frac{1 - e^{\lambda_k(t+\kappa)}}{\lambda_k} b_{T+\kappa} + \sigma_n \int_{-\infty}^t \alpha_k e^{\lambda_k(t-s)} dW_s \right] \quad (15) \end{aligned}$$

where $b_{T+\kappa}$ as in 10, and with x_0, x_1 are as in Theorem 1.

For a tempered stable subordinator, i.e., a non-negative BDLP, together with a non-negative kernel function (6) the resulting stationary CARMA process is non-negative. We could use the same approximation scheme as in (14). However, as Kawai (2017) noted, the Gaussian CARMA process would destroy its non-negativity. Therefore, we simulate $Y_t(\kappa, n) + \mathbb{E}[Q_t(n)] + \mathbb{E}[R_t(\kappa, n)]$ instead of discarding $Q_t(n)$ and $R_t(\kappa, n)$.

Scheme 2. Let $T > 0, \kappa > 0$. Let $p > 0, \alpha \in (0, 1)$. Let $\{L_t\}_{t \in \mathbb{R}}$ be a TS_{α}^p subordinator with Lévy measure M . Let $\bar{q} \leq \bar{p} - 1$ and let $a(z)$ and $b(z)$ be polynomials such that Assumption 1 is satisfied and α_k and λ_k for $k = 1, \dots, \bar{p}$ as in Lemma 1. Let $\{Y_t\}_{t \in \mathbb{R}}$ be a CARMA- p TS process. Let $n \in \mathbb{N}$. Let the random sequences be as in Scheme 1. Then, Y_t for $t \in [0, T]$ can be approximated by

$$\sum_{k=1}^{\bar{p}} \sum_{j=1}^{Z_{\kappa, n}} \alpha_k e^{\lambda_k(t-T_j)} \mathbb{1}_{(-\kappa, t]}(T_j) \left(\Lambda_{(j)}^{-1/\alpha} \wedge \frac{E_j^{1/p} U_j^{1/\alpha}}{\|V_j\|^{1/p}} \right) - \int_{\mathbb{R}_+} z (M - M_n)(dz) \frac{\alpha_k}{\lambda_k} - \int_{\mathbb{R}_+} z M_n(dz) \frac{\alpha_k}{\lambda_k} e^{\lambda_k(t+\kappa)}. \quad (16)$$

Remark 1. In Scheme 2, we can omit the term $\frac{V_j}{\|V_j\|}$ because for a subordinator the Lévy measure is only concentrated on \mathbb{R}_+ and thus numerator and denominator coincide.

Remark 2. As mentioned above, TS_α^p distributions are part of generalized tempered stable distributions of Rosiński & Sinclair (2010). In case of a generalized tempered stable distribution that is not in TS_α^p of course Theorem 1 does not apply anymore. However, Rosiński & Sinclair (2010) derived series representations with the inverse Lévy measure method and the rejection method. Then, (14), (15) and (16) are modified to contain the corresponding terms of the series of Theorems 5.1 and 5.5 in Rosiński & Sinclair (2010) (it is however necessary to check whether the generalized tempered stable distribution in question still fulfills the Wiener approximation assumption).

Remark 3. The proposed Scheme 2 can be extended to the case of multivariate CARMA processes (MCARMA) introduced in Marquardt & Stelzer (2007). In order to do so, we can replace Lemma 1 with its multivariate version in Proposition 5.1 of Schlemm & Stelzer (2012). Using this, a stationary MCARMA process can be expressed as a sum of dependent, complex-valued, and multivariate OU processes. The resulting formulas are lengthy and omitted but follow the same principle as in Scheme 2 above.

The above allows us to easily derive a bound for the approximation mean-squared error, which obviously depends on the specific underlying background-driving tempered stable process.

Corollary 1. *Under the assumptions of Scheme 1, let $\tilde{Y}_t(\kappa, n)$ denotes the approximation of Y_t according to (14) or (15). Then*

$$\begin{aligned} \mathbb{E} \left[(Y_t - \tilde{Y}_t(\kappa, n))^2 \right] &\leq -\sigma_n^2 \left(\sum_{k=1}^{\bar{p}} \frac{1}{2\lambda_k} \right) \left(\sum_{k=1}^{\bar{p}} \alpha_k^2 \right) + \left(\int_{\mathbb{R}} z(M - M_n)(dz) \right)^2 \left(\sum_{k=1}^{\bar{p}} \frac{\alpha_k}{\lambda_k} \right)^2 \\ &\quad - \int_{\mathbb{R}} z^2 M_n(dz) \left(\sum_{k=1}^{\bar{p}} \frac{e^{2\lambda_k(\kappa+t)}}{2\lambda_k} \right) \left(\sum_{k=1}^{\bar{p}} \alpha_k^2 \right) + \left(\int_{\mathbb{R}} z M_n(dz) \right)^2 \left(\sum_{k=1}^{\bar{p}} \frac{\alpha_k e^{\lambda_k(\kappa+t)}}{\lambda_k} \right)^2. \end{aligned} \quad (17)$$

If L is a subordinator as in Scheme 2 and $\tilde{Y}_t(\kappa, n)$ denote the approximation of Y_t according to (16), then

$$\mathbb{E} \left[(Y_t - \tilde{Y}_t(\kappa, n))^2 \right] \leq -\sigma_n^2 \left(\sum_{k=1}^{\bar{p}} \frac{1}{2\lambda_k} \right) \left(\sum_{k=1}^{\bar{p}} \alpha_k^2 \right) - \int_{\mathbb{R}_+} z^2 M_n(dz) \left(\sum_{k=1}^{\bar{p}} \frac{e^{2\lambda_k(\kappa+t)}}{2\lambda_k} \right) \left(\sum_{k=1}^{\bar{p}} \alpha_k^2 \right). \quad (18)$$

The formulas (17) and (18) appear unhandy but we can explicitly compute the error bounds for a specific parameter constellation with the help of the expressions for the first and second moments of the Lévy measure to be found in Appendix B.

5 Monte Carlo study

In this section, we conduct several Monte Carlo experiments to test the presented sampling routines. We follow up on the illustrative examples introduced earlier in Section 2. Unfortunately, there is no direct way to test whether a sample path was generated by a CARMA-pTS process. This is because the marginal distribution of a CARMA-pTS is not explicitly given. We therefore compare the empirical means and variances with their theoretical counterparts. Additionally, we inspect the empirical distribution of marginals given by the truncated series representation of a tempered stable Lévy process.

Example 1 (continuing from p.4). We start with the pTSS as the BDLP. We consider a range of parameter constellations to gauge the influence of different parameter values on the accuracy of our method. We choose $\alpha \in \{0.5, 0.8\}$, $p \in \{0.5, 1, 2\}$, $\delta = 1$ and $\lambda = 1$ as parameters for the pTSS. (In unreported results we see that the impact for scaling and tempering parameters is negligible.) To obtain a non-negative kernel function which fulfills Assumption 1 we set $\mathbf{a} = (3, 2)^T$ and $\mathbf{b} = (3, 1)^T$. We simulate paths on $[0, T]$ with $T = 100$. We make use of the decomposition $Y_t(\kappa, n) + \mathbb{E}[Q_t(n)] + \mathbb{E}[R_t(\kappa, n)]$ where $Y_t(\kappa, n)$ is the truncated series in (16) and $\mathbb{E}[Q_t(n)]$ and $\mathbb{E}[R_t(\kappa, n)]$ are the two remaining terms in (16). The expectations are analytically available. However, the formulas are lengthy and relegated to Appendix B. For $Y_t(\kappa, n)$, next to standard random sequences $\{E_j\}, \{U_j\}, \{T_j\}, \{\Lambda_j\}$, we need to simulate

$V_j \sim Q(dv)/\|\sigma\|$. In the present case, $\|\sigma\| = \delta = 1$ and thus $V_j = \lambda$ with probability 1. Therefore, $Y_t(\kappa, n)$ in (16) reduces to

$$\sum_{k=1}^2 \sum_{j=1}^{Z_{\kappa,n}} \alpha_k e^{\lambda_k(t-T_j)} \mathbf{1}_{(-\kappa, t]}(T_j) \left(\Lambda_{(j)}^{-1/\alpha} \wedge \frac{E_j^{1/p} U_j^{1/\alpha}}{\lambda^{1/p}} \right),$$

with $\lambda = 1$. For the above choice of \mathbf{a} and \mathbf{b} we have that $\alpha_1 = 2, \alpha_2 = -1, \lambda_1 = -1, \lambda_2 = -2$. We compare the accuracy for levels of truncation $n \in \{10, 100, 1000, 10000\}$. We set the threshold of jump times at $\kappa = 100$.

Figure 1 plots a typical paths of CARMA-pTSS process for $\alpha = 0.5, n = 10000, \kappa = 100$. The top panel shows a path for $p = 0.5$, the middle for $p = 1$ and the bottom for $p = 2$. The remaining parameters remain fixed at the aforementioned values. To ensure a fair comparison, we employ the same random sequence seed across all plots. We observe that for lower values of p , the path frequently traverses through smaller values, yet features higher peaks when compared to the paths corresponding to larger values of p . This observation aligns with an increase in the average value across the path as p increases.

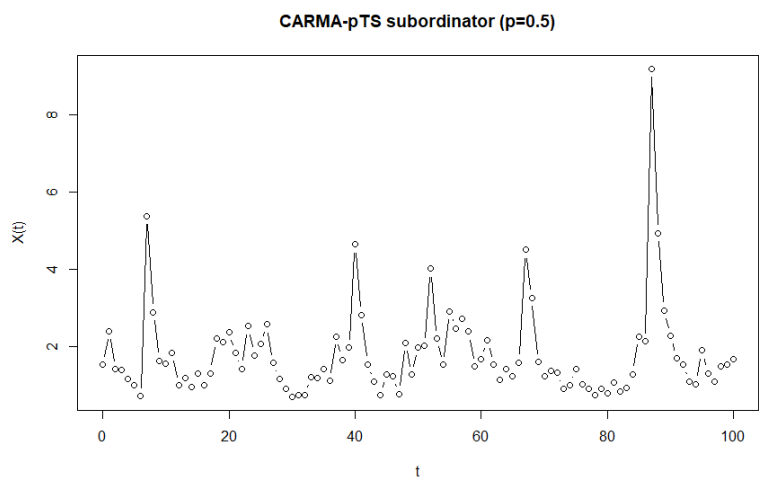
Table 1 reports absolute accuracy of Monte Carlo estimations of $\mathbb{E}[Y_t]$ and $\text{Var}[Y_t]$, both evaluated at times $t = 1$ and $t = 100$. We compare the said constellations for α, p and n . For each parameter constellation, we conduct simulations involving 10000 CARMA-pTSS paths. The empirical mean and empirical variance are subsequently computed. The table's two center columns report the absolute accuracies defined as $\widehat{\mathbb{E}}[Y_t] - \mathbb{E}[Y_t]$, and the two right-most report $\widehat{\text{Var}}[Y_t] - \text{Var}[Y_t]$. We make the following observations. The estimations are accurate in most cases for both expectation and variance. Interestingly, the estimation results do not improve for increasing n . The simulation performs well even for relatively small values of n . This phenomenon might be attributed to the fact that, given $T = \kappa = 100$, an average of 2000 jumps occurs per path for $n = 10$. This number of jumps seemingly suffices for Y_t to conform to its stationary distribution. We visualize this with Figure 2 which shows relative stability in the empirical density of Y_{100} realizations. Unfortunately, we cannot compare the empirical distributions with the true distribution due to the lack of a closed-form function. We omit figures for the other constellations of α and p because the pattern is the same.

The only exception with a worse accuracy is the case for $p = 0.5$ for the estimation of the variance. Remarkably, this behavior remains consistent across various values of n and persists for both examined α settings. This phenomenon can be attributed to the inherent nature of the problem: for small p values, seldom yet substantial spikes occur in the paths. Consequently, the accuracy of variance estimation is compromised due to these outliers. To visualize this, Figure 3 shows boxplots of the realizations of Y_{100} for $\alpha = 0.5$ and $n = 10000$ for the different p s.

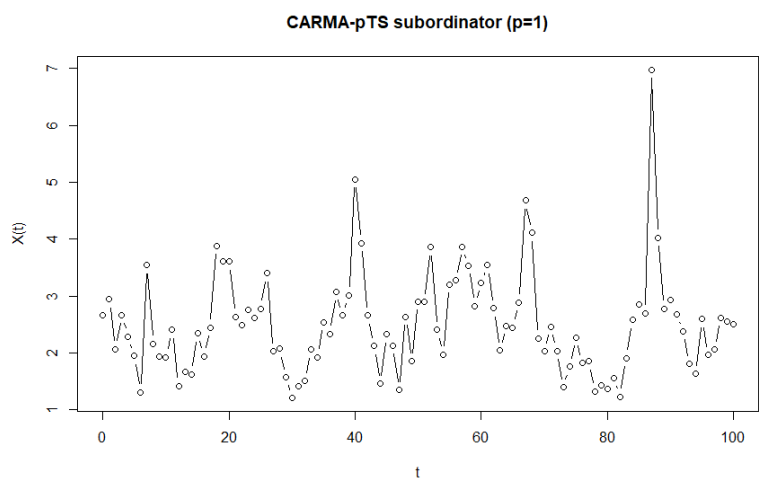
We extend the conducted simulation study to cases where $\kappa = 1$ and $\kappa = 10$, yielding qualitatively similar results, which are, however, omitted here for brevity. This demonstrates that for path simulations of a CARMA-pTSS process, modest values of n and κ turn out to be sufficient. Importantly, this is in contrast to the generation of i.i.d. tempered stable random variates through series representations. To illustrate this, we simulate 1000 i.i.d. random variates with a pTSS distribution for $p = 1$. We subsequently compare the empirical distributions across varying n values. Figure 4 plots the empirical densities for $\alpha = 0.5$ in panel (a) and $\alpha = 0.8$ in panel (b). For reference, the black solid line shows the true density function. As above, set $\delta = \lambda = 1$. As expected, the goodness-of-fit to the true distribution improves with increasing n . For $\alpha = 0.5$ a value of $n = 100$ seems to be sufficient. However, the situation changes considerably for $\alpha = 0.8$ where even a large value of $n = 100000$ fails to yield satisfactory goodness-of-fit results. For further comparison with the aforementioned Table 1, Table 2 reports the mean and variance accuracy for the i.i.d. case. We observe that while the simulated variates exhibit a variance close to the true one for $\alpha = 0.8$, there remains a substantial disparity in the mean, even for exceedingly large n values.

We also touch upon different series representations such as the rejection method of Rosiński & Sinclair (2010). We omit a full discussion and presenting lengthy tables because the differences in accuracy is not striking. The general observation is that the series representation of Section 4 has a slightly smaller numerical error than the rejection method of Rosiński & Sinclair (2010) which may also have the issue of a small number of non-rejections if n is small or if a high number of jumps is needed. The observations are in line with those of Imai & Kawai (2011) for $p = 1$.

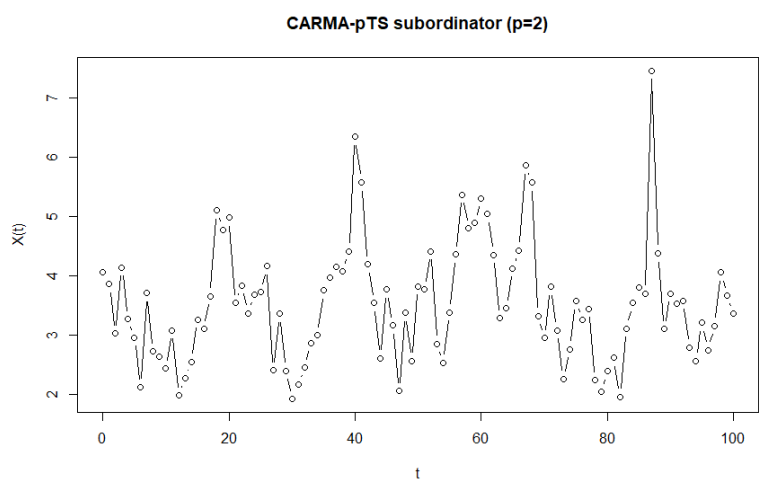
Example 2 (continuing from p. 4). We continue with the example of the pCTS distribution as the BDLP. As in Example 1, we set $T = \kappa = 100, \mathbf{a} = (3, 2)^T$ and $\mathbf{b} = (3, 1)^T$ and $p \in \{0.5, 1, 2\}$. In this instance, the parameters for the tempered stable distribution are $\delta_+ = \delta_- = \lambda_+ = \lambda_- = 1$ and $\alpha \in \{1.4, 1.8\}$. Given the symmetry of the measure Q for these parameter choices, we leverage (14) for simulation purposes. The sequence V_j is sampled such that $\mathbb{P}[V_j = -\lambda_-] = \mathbb{P}[V_j = +\lambda_+] = 0.5$. Figure 5 presents a typical



(a)



(b)



(c)

Figure 1: Sample paths of the CARMA-pTSS process for different p on $[0, 100]$. Other parameters fixed at $\alpha = 0.5, \delta = \lambda = 1, \mathbf{a} = (3, 2)^T, \mathbf{b} = (3, 1)^T$. We use (16) for simulation with $n = 10000, \kappa = 100$.

α	p	n	\mathbb{E}		$\mathbb{V}ar$	
			$t = 1$	$t = 100$	$t = 1$	$t = 100$
0.5	0.5	10	0.006	0.001	-0.165	0.397
		100	0.017	-0.001	0.063	0.511
		1000	-0.026	0.014	-0.013	0.078
		10000	0.026	0.009	0.174	0.126
	1	10	0.01	-0.004	0.001	-0.003
		100	-0.0003	0.002	0.013	-0.007
		1000	-0.011	0.013	-0.015	0.003
		10000	0.011	0.005	0.014	-0.011
	2	10	0.008	-0.001	0.007	-0.001
		100	-0.002	0.003	0.008	-0.008
		1000	-0.008	0.013	-0.013	0.006
		10000	0.007	0.006	0.003	-0.002
0.8	0.5	10	0.013	-0.007	-0.062	0.055
		100	0.022	0.011	0.196	0.179
		1000	-0.031	0.005	-0.144	0.231
		10000	0.026	0.012	0.2	0.261
	1	10	0.008	-0.006	-0.021	-0.028
		100	0.005	0.0006	0.024	-0.017
		1000	-0.01	0.006	-0.023	0.007
		10000	0.011	0.003	-0.002	0.0002
	2	10	0.006	-0.003	-0.024	-0.031
		100	0.01	-0.017	0.01	-0.017
		1000	-0.015	0.0005	-0.015	0.0005
		10000	-0.005	-0.003	-0.005	-0.003

Table 1: Accuracy estimations for expectations and variances based on 10000 sample paths of the CARMA-pTSS on $[0, 100]$ for different α and p . Other parameters fixed at $\delta = \lambda = 1$, $\mathbf{a} = (3, 2)^T$, $\mathbf{b} = (3, 1)^T$. We use (16) for simulation for different n with $\kappa = 100$.

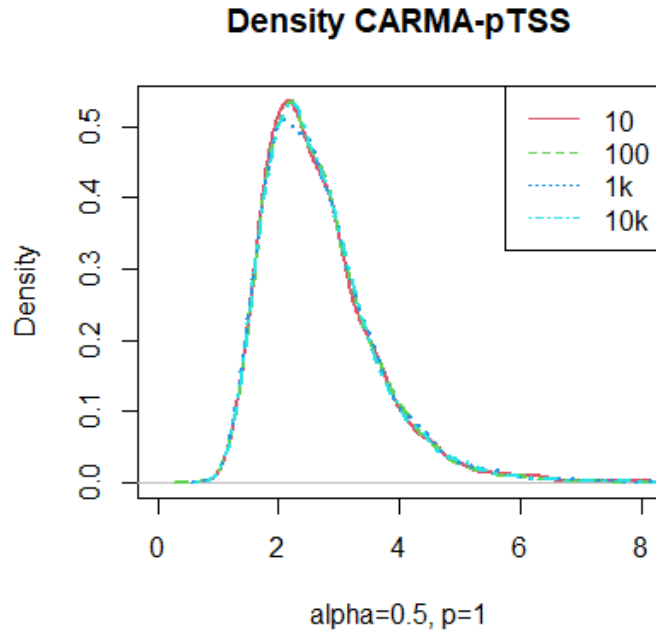


Figure 2: Empirical densities of 10000 realizations of Y_{100} of a CARMA-pTSS for different n . Parameters fixed $\alpha = 0.5$, $\delta = \lambda = 1$, $\mathbf{a} = (3, 2)^T$, $\mathbf{b} = (3, 1)^T$ and $\kappa = 100$.

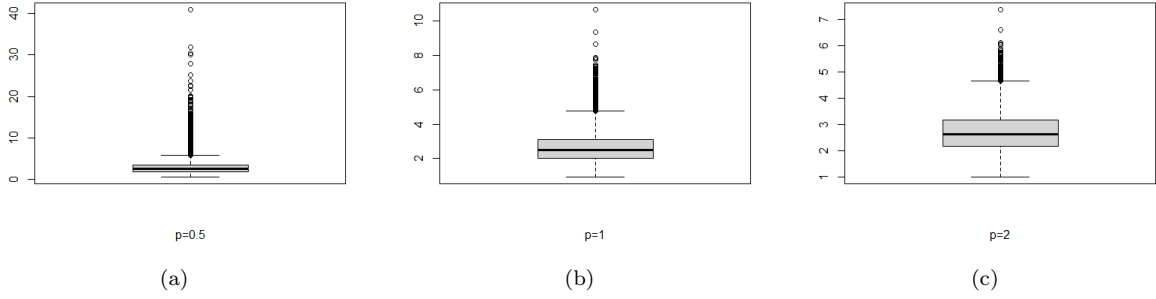


Figure 3: Boxplots of 10000 realizations of Y_{100} of a CARMA-pTSS for $p \in \{0.5, 1, 2\}$. Other parameters fixed $\alpha = 0.5, \delta = \lambda = 1, \mathbf{a} = (3, 2)^T, \mathbf{b} = (3, 1)^T$. We use $n = 10000, \kappa = 100$ for simulation.

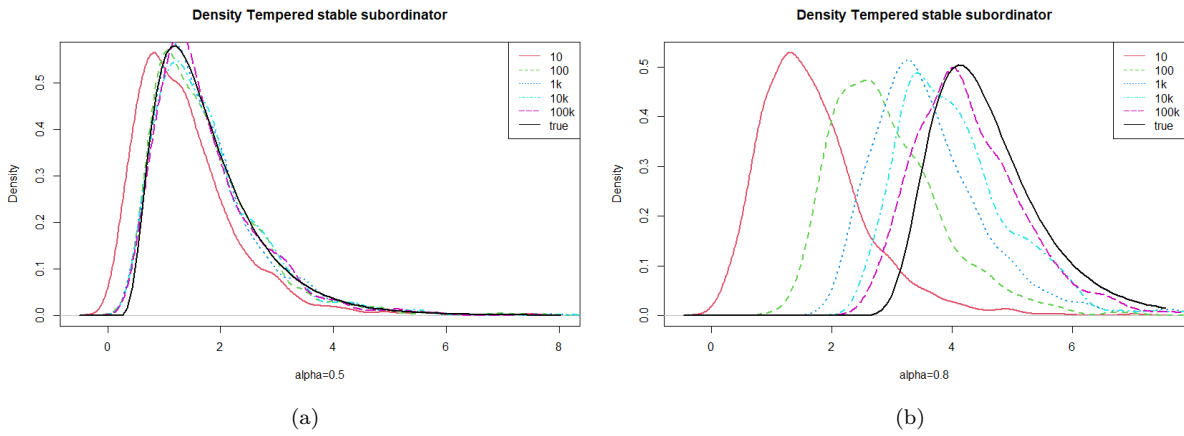


Figure 4: Empirical densities of 1000 i.i.d. realizations of a pTSS random variable for $\alpha \in \{0.5, 0.8\}$. Other parameters fixed $p = 1, \delta = \lambda = 1, \mathbf{a} = (3, 2)^T, \mathbf{b} = (3, 1)^T$. We compare different n and set $\kappa = 100$.

path for $\alpha = 1.4, p = 1$, and $n = 10000$.

Table 3 reports the estimated accuracy for both expectation and variance. The observations align with those made for CARMA-pTSS, with the additional insight that for $\alpha = 1.8$, variance estimation proves to be noisy across all considered values of p . This contrasts with Table 1 where this noisy behavior is only prevalent for $p = 0.5$.

Similarly to the previous example, we simulate i.i.d. random variates following the pCTS distribution.

α	n	\mathbb{E}	Var
0.5	10	-0.394	-0.095
	100	-0.038	0.073
	1000	-0.035	0.006
	10000	-0.01	-0.014
	100000	-0.03	-0.063
0.8	10	-2.913	-0.164
	100	-1.648	0.097
	1000	-0.977	-0.003
	10000	-0.533	0.043
	100000	-0.312	-0.094

Table 2: Accuracy estimations for expectations and variances based on 1000 i.i.d. realizations of a pTSS random variable for $\alpha \in \{0.5, 0.8\}$. Other parameters fixed $p = 1, \delta = \lambda = 1, \mathbf{a} = (3, 2)^T, \mathbf{b} = (3, 1)^T$. We compare different n and set $\kappa = 100$.

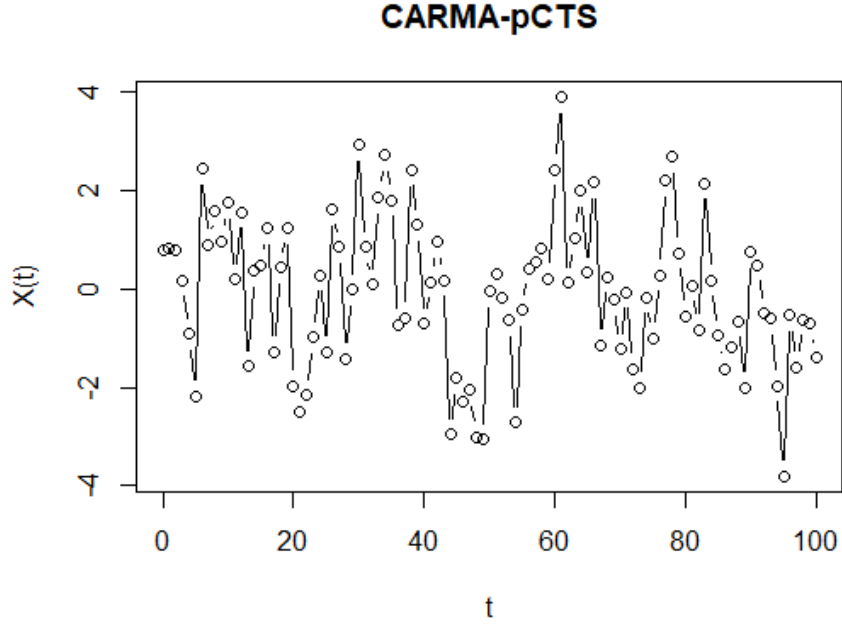


Figure 5: Sample paths of the CARMA-pCTS process on $[0, 100]$. Parameters fixed at $\alpha = 1.4, p = \delta_+ = \delta_- = \lambda_+ = \lambda_- = 1, \mathbf{a} = (3, 2)^T, \mathbf{b} = (3, 1)^T$. We use (14) for simulation with $n = 10000, \kappa = 100$.

α	p	n	\mathbb{E}		Var	
			$t = 1$	$t = 100$	$t = 1$	$t = 100$
1.4	0.5	10	0.022	0.006	0.145	-0.09
		100	-0.021	0.004	-0.03	-0.029
		1000	-0.005	-0.008	-0.032	0.066
		10000	-0.021	0.005	-0.055	0.354
	1	10	0.01	0.006	0.005	-0.018
		100	-0.012	0.009	0.024	-0.059
		1000	-0.002	-0.01	-0.048	0.065
		10000	-0.02	-0.005	-0.0005	0.07
	2	10	0.006	0.006	0.007	-0.011
		100	-0.008	0.009	0.03	-0.065
		1000	-0.003	-0.014	-0.042	0.034
		10000	-0.022	-0.011	-0.005	0.058
1.8	0.5	10	0.009	0.017	0.12	-0.099
		100	-0.041	0.011	-0.164	-0.043
		1000	0.013	-0.016	-0.07	0.287
		10000	-0.013	0.018	0.132	0.321
	1	10	0.001	0.013	0.076	-0.065
		100	-0.038	0.014	-0.149	-0.162
		1000	0.017	-0.021	-0.025	0.24
		10000	-0.02	0.005	0.151	0.257
	2	10	-0.002	0.013	0.08	-0.052
		100	-0.033	0.017	-0.13	-0.173
		1000	0.016	-0.025	-0.002	0.192
		10000	-0.023	-0.005	0.147	0.22

Table 3: Accuracy estimations for expectations and variances based on 10000 sample paths of the CARMA-pCTS on $[0, 100]$ for different α and p . Other parameters fixed at $\delta_+ = \delta_- = \lambda_+ = \lambda_- = 1, \mathbf{a} = (3, 2)^T, \mathbf{b} = (3, 1)^T$. We use (14) for simulation for different n with $\kappa = 100$.

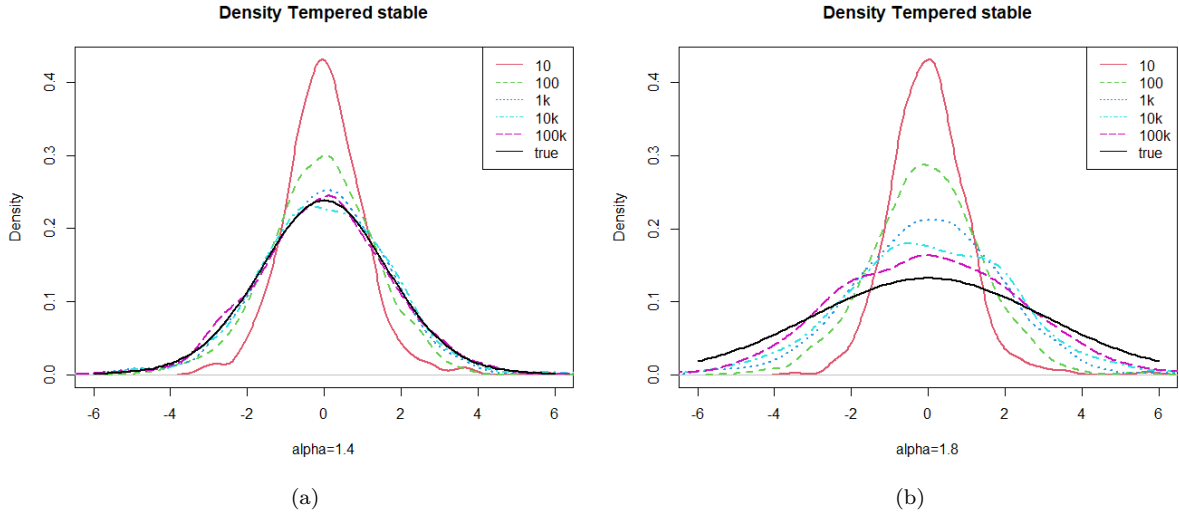


Figure 6: Empirical densities of 1000 i.i.d. realizations of a pCTS random variable for $\alpha \in \{1.4, 1.8\}$. Other parameters fixed $p = 1, \delta_+ = \delta_- = \lambda_+ = \lambda_- = 1, \mathbf{a} = (3, 2)^\top, \mathbf{b} = (3, 1)^\top$. We compare different n and set $\kappa = 100$.

We compare the empirical distribution with the theoretical counterpart. Let $\alpha \in \{1.4, 1.8\}$ and set $p = 1$ and all remaining parameters as above. Table 6 and Figure 4 collect the results. We again observe as α increases the goodness-of-fit of the empirical distribution diminishes for fixed n . While $n = 10000$ seems adequate for $\alpha = 1.4$, even $n = 100000$ fails to generate satisfactory random variates for $\alpha = 1.8$. However, note that there are other simulation approaches for the CTS distribution for $\alpha \in (1, 2)$, e.g., Kawai & Masuda (2011b) propose an approximate acceptance-rejection algorithm.

α	n	\mathbb{E}	$\mathbb{V}ar$
0.5	10	0.0005	-1.882
	100	-0.057	-1.056
	1000	-0.007	-0.305
	10000	0.047	-0.03
	100000	-0.032	-0.085
0.8	10	0.0004	-8.221
	100	-0.054	-7.15
	1000	-0.004	-5.71
	10000	0.073	-4.399
	100000	-0.016	-3.72

Table 4: Accuracy estimations for expectations and variances based on 1000 i.i.d. realizations of a pCTS random variable for $\alpha \in \{1.4, 1.8\}$. Other parameters fixed $p = 1, \delta_+ = \delta_- = \lambda_+ = \lambda_- = 1, \mathbf{a} = (3, 2)^\top, \mathbf{b} = (3, 1)^\top$. We compare different n and set $\kappa = 100$.

Example 3 (continuing from p. 4). Lastly, we turn to the case of the CARMA-p Γ TS process. Again, we set $T = \kappa = 100, \mathbf{a} = (3, 2)^\top$ and $\mathbf{b} = (3, 1)^\top$ and $p \in \{0.5, 1, 2\}$. Additionally, we set $\beta = 3, \lambda = 1$ and $\alpha \in \{0.5, 0.8\}$. Given that $\|\sigma\| = 1, \tilde{Q} = \Gamma(\beta/p, \lambda)$ and thus it is a standard task to sample $\{V_j\}$. Because we are dealing with a subordinator we can use (16) to sample paths. Formulas for the expectations in (16) are cumbersome and relegated to Appendix B. Figure 7 shows a typical path for $\alpha = 0.5, p = 1, n = 10000$. Table 5 reports the estimated accuracy for expectation and variance. Unlike in the other examples, there appears to be no trend of less accurate variance estimation for small values of p in this instance.

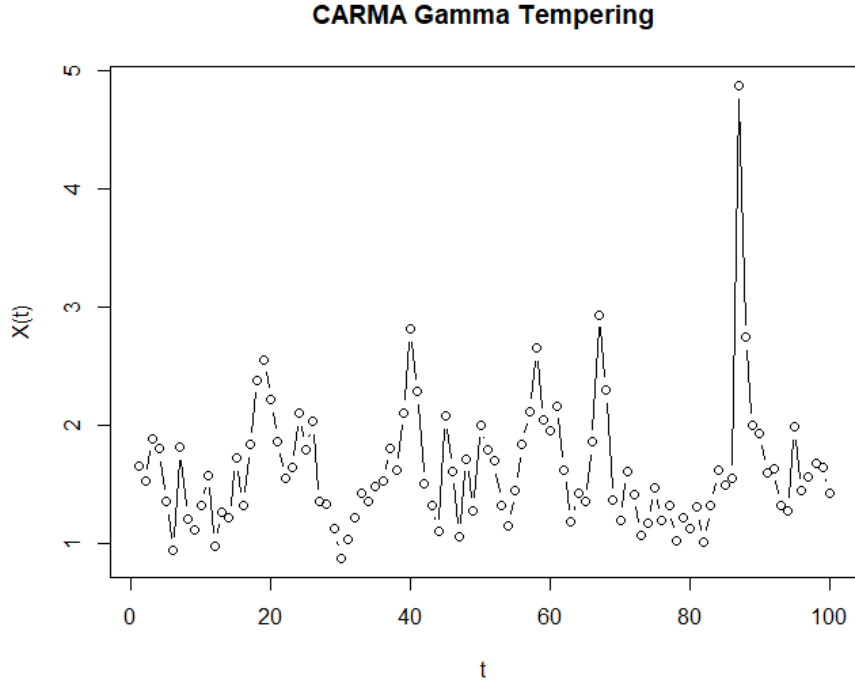


Figure 7: Sample paths of the CARMA-pΓTS process on $[0, 100]$. Parameters fixed at $\alpha = 0.5, p = 1, \beta = 3, \lambda = 1, \mathbf{a} = (3, 2)^T, \mathbf{b} = (3, 1)^T$. We use (16) for simulation with $n = 10000, \kappa = 100$.

α	p	n	\mathbb{E}		Var	
			$t = 1$	$t = 100$	$t = 1$	$t = 100$
0,5	0,5	10	0,003	-0,001	0,017	0,001
		100	-0,0002	-0,0003	-0,005	-0,007
		1000	-0,002	0,001	-0,009	-0,005
		10000	0,001	0,002	-0,003	-0,008
	1	10	0,002	-0,003	-0,016	0,025
		100	-0,001	0,004	-0,008	0,039
		1000	-0,004	0,01	-0,014	0,006
		10000	0,009	0,001	0,02	-0,019
	2	10	0,011	0,006	0,01	0,022
		100	-0,001	-0,004	-0,011	-0,035
		1000	-0,012	0,01	-0,015	-0,02
		10000	0,006	0,013	-0,004	0,011
0,8	0,5	10	0,002	-0,001	-0,013	-0,007
		100	0,001	0,001	-0,002	-0,002
		1000	-0,001	0,001	-0,002	0,004
		10000	-0,0000	0,002	-0,005	-0,001
	1	10	-0,001	-0,001	-0,03	0,013
		100	0,001	0,004	0,003	0,05
		1000	-0,004	0,008	-0,008	0,027
		10000	0,01	0,002	0,011	-0,007
	2	10	0,006	0,001	-0,034	-0,026
		100	-0,0004	-0,002	0,003	-0,022
		1000	-0,015	0,006	-0,049	-0,001
		10000	0,005	0,007	-0,0002	-0,003

Table 5: Accuracy estimations for expectations and variances based on 10000 sample paths of the CARMA-pΓTS on $[0, 100]$ for different α and p . Other parameters fixed at $\beta = 3, \lambda = 1, \mathbf{a} = (3, 2)^T, \mathbf{b} = (3, 1)^T$. We use (16) for simulation for different n with $\kappa = 100$.

6 Conclusion

In this paper, we conducted a comprehensive analysis of simulation techniques for p -tempered α -stable Lévy processes, with a specific focus on CARMA processes driven by such Lévy processes. We have shown a series representation result and propose a simulation scheme for CARMA-pTS processes based on Kawai (2017) and truncated series representations. We found a representation for the error. In a simulation study we observed the efficacy of our proposed scheme in practical applications for a small level of truncation. Remarkably, our simulation method displayed higher accuracy compared to the simulation of the background-driving Lévy process itself. An interesting direction for future research is the simultaneous estimation of the parameters α and p to make TS_α^p distributions more accessible for financial researchers. Further topics also include generalizations of CARMA processes as volatility modulated Volterra processes (Barndorff-Nielsen et al. 2013).

Acknowledgements

Financial support of the German Research Foundation (Deutsche Forschungsgemeinschaft, DFG) via the project 455257011 is gratefully acknowledged.

The author is grateful to two anonymous referees as well as Christoph Hanck for valuable comments which helped to substantially improve this paper. Full responsibility is taken for all remaining errors.

References

- Barndorff-Nielsen, O. E., Benth, F. E. & Veraart, A. E. (2013), ‘Modelling energy spot prices by volatility modulated Lévy-driven Volterra processes’, *Bernoulli* **19**(3), 803–845.
- Barndorff-Nielsen, O. E. & Shephard, N. (2001), ‘Non-Gaussian Ornstein–Uhlenbeck-based models and some of their uses in financial economics’, *Journal of the Royal Statistical Society: Series B (Statistical Methodology)* **63**(2), 167–241.
- Bianchi, M. L., Rachev, S. T., Kim, Y. S. & Fabozzi, F. J. (2011), ‘Tempered infinitely divisible distributions and processes’, *Theory of Probability & Its Applications* **55**(1), 2–26.
URL: <https://doi.org/10.1137/S0040585X97984632>
- Brockwell, P. (1994), ‘On continuous-time threshold ARMA processes’, *Journal of Statistical Planning and Inference* **39**(2), 291–303.
URL: <https://www.sciencedirect.com/science/article/pii/0378375894902100>
- Brockwell, P. (2014), ‘Recent results in the theory and applications of CARMA processes’, *Annals of the Institute of Statistical Mathematics* **66**, 647–685.
- Brockwell, P. J. (2001), ‘Lévy-driven CARMA processes’, *Annals of the Institute of Statistical Mathematics* **53**(1), 113–124.
URL: <https://doi.org/10.1023/A:1017972605872>
- Brockwell, P. J., Davis, R. A. & Yang, Y. (2011), ‘Estimation for non-negative Lévy-driven CARMA processes’, *Journal of Business & Economic Statistics* **29**(2), 250–259.
URL: <https://doi.org/10.1198/jbes.2010.08165>
- Carr, P., Geman, H., Madan, D. B. & Yor, M. (2002), ‘The fine structure of asset returns: An empirical investigation’, *The Journal of Business* **75**(2), 305–332.
URL: <https://doi.org/10.1086/338705>
- Cohen, S. & Rosiński, J. (2007), ‘Gaussian Approximation of Multivariate Lévy Processes with Applications to Simulation of Tempered Stable Processes’, *Bernoulli* **13**(1), 195–210.
URL: <http://dx.doi.org/10.3150/07-BEJ6011>
- Fallahgoul, H. & Loeper, G. (2019), ‘Modelling tail risk with tempered stable distributions: an overview’, *Annals of Operations Research* pp. 1–28.
URL: <https://doi.org/10.1007/s10479-019-03204-3>

- Grabchak, M. (2012), ‘On a new class of tempered stable distributions: moments and regular variation’, *Journal of Applied Probability* **49**(4), 1015–1035.
 URL: <https://doi.org/10.1239/jap/1354716655>
- Grabchak, M. (2016), *Tempered Stable Distributions: Stochastic Models for Multiscale Processes*, Springer.
 URL: <https://doi.org/10.1007/978-3-319-24927-8>
- Grabchak, M. (2019), ‘Rejection sampling for tempered Lévy processes’, *Statistics and Computing* **29**(3), 549–558.
 URL: <https://doi.org/10.1007/s11222-018-9822-6>
- Grabchak, M. & Sabino, P. (2023), ‘Efficient simulation of p -tempered α -stable OU processes’, *Statistics and Computing* **33**(1), 4.
 URL: <https://doi.org/10.1007/s11222-022-10165-4>
- Imai, J. & Kawai, R. (2011), ‘On finite truncation of infinite shot noise series representation of tempered stable laws’, *Physica A: Statistical Mechanics and its Applications* **390**(23), 4411 – 4425.
 URL: <http://www.sciencedirect.com/science/article/pii/S0378437111005759>
- Imai, J. & Kawai, R. (2013), ‘Numerical inverse Lévy measure method for infinite shot noise series representation’, *Journal of Computational and Applied Mathematics* **253**, 264–283.
 URL: <http://dx.doi.org/10.1016/j.cam.2013.04.003>
- Kawai, R. (2017), ‘Sample path generation of Lévy-driven continuous-time autoregressive moving average processes’, *Methodology and Computing in Applied Probability* **19**(1), 175–211.
 URL: <https://doi.org/10.1007/s11009-015-9472-5>
- Kawai, R. (2021), ‘A general approach to sample path generation of infinitely divisible processes via shot noise representation’, *Statistics & Probability Letters* **174**, 109091.
- Kawai, R. & Masuda, H. (2011a), ‘Exact discrete sampling of finite variation tempered stable Ornstein–Uhlenbeck processes’, *Monte Carlo Methods and Applications* **17**(3), 279–300.
 URL: <https://doi.org/10.1515/mcma.2011.012>
- Kawai, R. & Masuda, H. (2011b), ‘On simulation of tempered stable random variates’, *Journal of Computational and Applied Mathematics* **235**(8), 2873–2887.
 URL: <https://doi.org/10.1016/j.cam.2010.12.014>
- Kim, Y. S., Rachev, S. T., Bianchi, M. L. & Fabozzi, F. J. (2008), ‘Financial market models with Lévy processes and time-varying volatility’, *Journal of Banking & Finance* **32**(7), 1363–1378.
 URL: <https://doi.org/10.1016/j.jbankfin.2007.11.004>
- Koponen, I. (1995), ‘Analytic approach to the problem of convergence of truncated Lévy flights towards the gaussian stochastic process’, *Physical Review E* **52**(1), 1197.
 URL: <https://doi.org/10.1103/PhysRevE.52.1197>
- Marquardt, T. & Stelzer, R. (2007), ‘Multivariate CARMA processes’, *Stochastic Processes and their Applications* **117**(1), 96–120.
- Qu, Y., Dassios, A. & Zhao, H. (2021), ‘Exact simulation of Ornstein–Uhlenbeck tempered stable processes’, *Journal of Applied Probability* **58**(2), 347–371.
 URL: <https://doi.org/10.1017/jpr.2020.92>
- Rachev, S., Kim, Y., Bianchi, M. & Fabozzi, F. (2011), *Financial Models with Levy Processes and Volatility Clustering*, Frank J. Fabozzi Series, Wiley.
 URL: https://books.google.de/books?id=XKvUUrC5_twC
- Rosiński, J. (2001), Series representations of Lévy processes from the perspective of point processes, in O. E. Barndorff-Nielsen, S. I. Resnick & T. Mikosch, eds, ‘Lévy Processes: Theory and Applications’, Birkhäuser, Boston, pp. 401–415.
 URL: https://doi.org/10.1007/978-1-4612-0197-7_18
- Rosiński, J. (2007), ‘Tempering stable processes’, *Stochastic processes and their applications* **117**(6), 677–707.
 URL: <https://doi.org/10.1016/j.spa.2006.10.003>

- Rosiński, J. & Sinclair, J. (2010), ‘Generalized tempered stable processes’, *Stability in Probability* **90**, 153–170.
URL: <http://eudml.org/doc/281880>
- Sabino, P. (2022), ‘Exact simulation of normal tempered stable processes of OU type with applications’, *Statistics and Computing* **32**(5), 81.
- Sabino, P. & Petroni, N. C. (2022), ‘Fast simulation of tempered stable Ornstein–Uhlenbeck processes’, *Computational Statistics* **37**(5), 2517–2551.
URL: <https://doi.org/10.1007/s00180-022-01205-8>
- Schlemm, E. & Stelzer, R. (2012), ‘Multivariate CARMA processes, continuous-time state space models and complete regularity of the innovations of the sampled processes’, *Bernoulli* **18**(1), 46–63.
- Terdik, G. & Woyczynski, W. (2006), ‘Rosinski measures for tempered stable and related Ornstein–Uhlenbeck processes’, *Probability and Mathematical Statistics* **26**(2), 213.
- Todorov, V. & Tauchen, G. (2006), ‘Simulation Methods for Lévy-Driven Continuous-Time Autoregressive Moving Average (CARMA) Stochastic Volatility Models’, *Journal of Business & Economic Statistics* **24**(4), 455–469.
URL: <http://dx.doi.org/10.1198/073500106000000260>
- Tweedie, M. C. (1984), An index which distinguishes between some important exponential families, *in* ‘Statistics: Applications and new directions: Proc. Indian statistical institute golden Jubilee International conference’, Vol. 579, pp. 579–604.
- Yuan, S. & Kawai, R. (2021), ‘Numerical aspects of shot noise representation of infinitely divisible laws and related processes’, *Probability Surveys* **18**, 201–271.
- Zhang, S. & Zhang, X. (2009), ‘On the transition law of tempered stable Ornstein–Uhlenbeck processes’, *Journal of Applied Probability* **46**(3), 721–731.
URL: <https://doi.org/10.1239/jap/1253279848>

A Appendix: Proofs

Proof of Theorem 1. We extend the proofs of Rosiński (2007) and Bianchi et al. (2011). As in Rosiński (2001), it is enough to prove the statements for fixed t . Define

$$H(\Gamma_j; (V_j, E_j, U_j)) := \left(\left(\frac{\alpha \Gamma_j}{\|\sigma\|T} \right)^{-1/\alpha} \wedge \frac{E_j^{1/p} U_j^{1/\alpha}}{\|V_j\|^{1/p}} \right) \frac{V_j}{\|V_j\|}. \quad (19)$$

We need to show

$$\int_0^\infty \mathbb{P} \left[\mathbf{1}_{(0,t]}(T_j) H(s; (V_j, E_j, U_j)) \in A \right] = tM(A) \quad (20)$$

for every $0 \notin A \in \mathcal{B}(\mathbb{R}^d)$. It is enough to verify (20) for sets of the form $A = \{x \in \mathbb{R} : \|x\| > a, \frac{x}{\|x\|} \in B\}$, where $a > 0$ and $B \in \mathcal{B}(\mathbb{S}^{d-1})$. For such A the left-hand-side of (20) can be written as

$$\begin{aligned} & \int_0^\infty \mathbb{P} [T_j \in (0, t]] \mathbb{P} \left[\left(\left(\frac{\alpha \Gamma_j}{\|\sigma\|T} \right)^{-1/\alpha} \wedge \frac{E_j^{1/p} U_j^{1/\alpha}}{\|V_j\|^{1/p}} \right) \frac{V_j}{\|V_j\|} \in A \right] ds \\ &= \frac{t}{T} \mathbb{E} \left[\int_0^\infty \mathbf{1} \left(\left(\frac{\alpha \Gamma_j}{\|\sigma\|T} \right)^{-1/\alpha} > a, E_j^{1/p} U_j^{1/\alpha} > a \|V_j\|^{1/p}, \frac{V_j}{\|V_j\|} \in B \right) ds \right] \\ &= t\alpha^{-1} \|\sigma\| a^{-\alpha} \mathbb{E} \left[\mathbf{1} \left(E_j^{1/p} U_j^{1/\alpha} > a \|V_j\|^{1/p}, \frac{V_j}{\|V_j\|} \in B \right) \right] \\ &= t\alpha^{-1} a^{-\alpha} \int_B \int_0^\infty \mathbb{P} \left[E_j^{1/p} U_j^{1/\alpha} > a \|V_j\|^{1/p} \right] Q(ds|u) \sigma(du) \end{aligned}$$

$$\begin{aligned}
&= t \int_B \int_0^\infty \int_a^\infty e^{-r^p s} r^{-\alpha-1} dr Q(ds|u) \sigma(du) \\
&= t \int_B \int_a^\infty q(r^p, u) dr \sigma(du) \\
&= tM(A),
\end{aligned}$$

where the fourth inequality follows by conditioning and integration by substitution,

$$\mathbb{P} \left[E_j^{1/p} U_j^{1/\alpha} > a \|V_j\|^{1/p} \right] = \int_0^1 e^{-\frac{a^p s}{x^{p/\alpha}}} dx = a^\alpha \alpha \int_a^\infty e^{-r^p s} r^{-\alpha-1} dr.$$

This proves (20).

For $\alpha \in (0, 1)$ or Q is symmetric and $\alpha \in [1, 2)$, the remainder of the proof is exactly as in Rosiński (2007) which proves (i). For (ii), first consider the case $\alpha \in (1, 2)$. We need to show

$$\sum_{j=1}^\infty \frac{t}{T} \left(\frac{\alpha j}{\|\sigma\|T} \right)^{-1/\alpha} x_0 - \frac{t}{T} c_j = t b_T,$$

where

$$c_j = \int_{j-1}^j \mathbb{E} \left[\left(\left(\frac{\alpha s}{\|\sigma\|T} \right)^{-1/\alpha} \wedge \frac{E_j^{1/p} U_j^{1/\alpha}}{\|V_j\|^{1/p}} \right) \frac{V_j}{\|V_j\|} \right] ds$$

and b_T as in (10).

Define as in Rosiński (2007)

$$c'_j = \int_{j-1}^j \mathbb{E} \left[\left(\frac{\alpha s}{\|\sigma\|T} \right)^{-1/\alpha} \frac{V_j}{\|V_j\|} \right] ds = \frac{\alpha^{1-1/\alpha} (\|\sigma\|T)^{1/\alpha}}{\alpha-1} (j^{1-1/\alpha} - (j-1)^{1-1/\alpha}) x_0,$$

for $j \geq 1$. The procedure now is analogously to Rosiński (2007) by first showing absolute summability of $\|c'_j - c_j\|$ and then computing $\sum_{j=1}^\infty (c'_j - c_j)$. We only have to replace $\mathbb{E}[E_1^{(1-\alpha)}]$ by $\mathbb{E}[E_1^{(1-\alpha)/p}] = \Gamma\left(\frac{1+p-\alpha}{p}\right)$ in each step and use the conversion rule (3) for general p .

For $\alpha = 1$, we again follow Rosiński (2007) and replace $\mathbb{E}[\log(E_1 U_1)]$ by $\mathbb{E}[\log(E_1^{1/p} U_1)] = -1 - \gamma/p$ in each step. This completes the proof. \square

Proof of Theorem 2. Theorem 1 implies that

$$M((x, \infty)B) = \int_{\mathbb{R}^d} \int_0^\infty \int_0^1 \int_0^\infty \mathbf{1}_{(x, \infty)} \left(\left(\frac{\alpha s}{\|\sigma\|} \right)^{-1/\alpha} \wedge \frac{r^{1/p} u^{1/\alpha}}{\|v\|^{1/p}} \right) \mathbf{1}_B \left(\frac{v}{\|v\|} \right) ds du e^{-r} dr \tilde{Q}(dv),$$

for $x > 0$ and $B \in \mathcal{B}(\mathbb{S}^{d-1})$, where $\tilde{Q}(dv) := Q(dv)/\|\sigma\|$.

As in Imai & Kawai (2011),

$$\begin{aligned}
&\int_0^n \mathbf{1}_{(x, \infty)} \left(\left(\frac{\alpha s}{\|\sigma\|} \right)^{-1/\alpha} \wedge \frac{r^{1/p} u^{1/\alpha}}{\|v\|^{1/p}} \right) \\
&= \mathbf{1}_{(x, \infty)} \left(\frac{r^{1/p} u^{1/\alpha}}{\|v\|^{1/p}} \right) \text{Leb} \left(\left\{ s \in (0, n) \left(\frac{\alpha s}{\|\sigma\|} \right)^{-1/\alpha} > x \right\} \right) \\
&= \mathbf{1}_{(x, \infty)} \left(\frac{r^{1/p} u^{1/\alpha}}{\|v\|^{1/p}} \right) \left(n \wedge \frac{\|\sigma\|}{\alpha} x^{-\alpha} \right).
\end{aligned}$$

Due to the truncation, $L^{(n)}$ has the triplet $(0, 0, M_n)$, where

$$M_n((x, \infty)B) = \int_{\mathbb{R}^d} \int_0^\infty \int_0^1 \int_0^n \mathbf{1}_{(x, \infty)} \left(\left(\frac{\alpha s}{\|\sigma\|} \right)^{-1/\alpha} \wedge \frac{r^{1/p} u^{1/\alpha}}{\|v\|^{1/p}} \right) \mathbf{1}_B \left(\frac{v}{\|v\|} \right) ds du e^{-r} dr \tilde{Q}(dv)$$

$$\begin{aligned}
&= \int_{\mathbb{R}^d} \int_0^\infty \int_0^1 \mathbf{1}_{(x,\infty)} \left(\frac{r^{1/p} u^{1/\alpha}}{\|v\|^{1/p}} \right) \left(n \wedge \frac{\|\sigma\|}{\alpha} x^{-\alpha} \right) \mathbf{1}_B \left(\frac{v}{\|v\|} \right) \mathrm{d}u e^{-r} \mathrm{d}r \tilde{Q}(dv) \\
&= \left(n \frac{\alpha}{\|\sigma\|} x^\alpha \wedge 1 \right) \int_{\mathbb{R}^d} \int_0^\infty \int_0^1 \mathbf{1}_{(x,\infty)} \left(\frac{r^{1/p} u^{1/\alpha}}{\|v\|^{1/p}} \right) \frac{\|\sigma\|}{\alpha} x^{-\alpha} \mathbf{1}_B \left(\frac{v}{\|v\|} \right) \mathrm{d}u e^{-r} \mathrm{d}r \tilde{Q}(dv) \\
&= \left(n \frac{\alpha}{\|\sigma\|} x^\alpha \wedge 1 \right) \int_{\mathbb{R}^d} \int_0^\infty \int_0^1 \int_0^\infty \mathbf{1}_{(x,\infty)} \left(\left(\frac{\alpha s}{\|\sigma\|} \right)^{-1/\alpha} \wedge \frac{r^{1/p} u^{1/\alpha}}{\|v\|^{1/p}} \right) \mathbf{1}_B \left(\frac{v}{\|v\|} \right) \mathrm{d}s \mathrm{d}u e^{-r} \mathrm{d}r \tilde{Q}(dv) \\
&= \left(n \frac{\alpha}{\|\sigma\|} x^\alpha \wedge 1 \right) M((x, \infty)B).
\end{aligned}$$

The fourth inequality follows since, analogously to Imai & Kawai (2011),

$$\mathbf{1}_{(x,\infty)} \left(\frac{r^{1/p} u^{1/\alpha}}{\|v\|^{1/p}} \right) \frac{\|\sigma\|}{\alpha} x^{-\alpha} = \int_0^\infty \mathbf{1}_{(x,\infty)} \left(\left(\frac{\alpha s}{\|\sigma\|} \right)^{-1/\alpha} \wedge \frac{r^{1/p} u^{1/\alpha}}{\|v\|^{1/p}} \right) \mathrm{d}s.$$

□

Proof of Corollary 1. For the first,

$$\begin{aligned}
\mathbb{E} \left[(Y_t - \tilde{Y}_t(\kappa, n))^2 \right] &\leq \mathbb{E}[Q_t(n)^2] + \mathbb{E}[R_t(\kappa, n)^2] \\
&= \mathrm{Var}[Q_t(n)] + \mathbb{E}[Q_t(n)]^2 + \mathrm{Var}[R_t(\kappa, n)] + \mathbb{E}[R_t(\kappa, n)]^2.
\end{aligned}$$

We have by the definitions

$$\begin{aligned}
\mathbb{E}[Q_t(n)] &= \int_{\mathbb{R}} z(M - M_n)(dz) \int_{-\infty}^T g(t-s) \mathrm{d}s = - \int_{\mathbb{R}} z(M - M_n)(dz) \sum_{k=1}^{\bar{p}} \frac{\alpha_k}{\lambda_k}, \\
\mathbb{E}[R_t(\kappa, n)] &= \int_{\mathbb{R}} M_n(dz) \int_{-\infty}^{-\kappa} g(t-s) \mathrm{d}s = - \int_{\mathbb{R}} M_n(dz) \sum_{k=1}^{\bar{p}} \frac{\alpha_k e^{\lambda_k(\kappa+t)}}{\lambda_k},
\end{aligned}$$

and

$$\begin{aligned}
\mathrm{Var}[Q_t(n)] &= \int_{\mathbb{R}} z^2(M - M_n)(dz) \int_{-\infty}^T g(t-s)^2 \mathrm{d}s \leq -\sigma_n^2 \left(\sum_{k=1}^{\bar{p}} \frac{1}{2\lambda_k} \right) \left(\sum_{k=1}^{\bar{p}} \alpha_k^2 \right), \\
\mathrm{Var}[R_t(\kappa, n)] &= \int_{\mathbb{R}} z^2 M_n(dz) \int_{-\infty}^{-\kappa} g(t-s)^2 \mathrm{d}s \leq - \int_{\mathbb{R}} z^2 M_n(dz) \left(\sum_{k=1}^{\bar{p}} \frac{e^{2\lambda_k(\kappa+t)}}{2\lambda_k} \right) \left(\sum_{k=1}^{\bar{p}} \alpha_k^2 \right),
\end{aligned}$$

where we have used the Cauchy-Schwarz inequality. This implies the first result. With this, the second is straightforward. □

B Appendix: Lévy measure moments

We collect formulas of the truncated Lévy measure, i.e.,

$$\int z M_n(dz) \quad \text{and} \quad \int z^2 M_n(dz)$$

for our examples. With these it is computationally straight-forward to derive $\mathbb{E}[Q_t(n)]$, $\mathbb{E}[R_t(\kappa, n)]$, $\mathrm{Var}[Q_t(n)]$, and $\mathrm{Var}[R_t(\kappa, n)]$.

Example 1 (continuing from p. 4). With the help of (11), we obtain for the pTSS

$$\int_0^\infty z M_n(dz) = \alpha n \left(\left(\frac{\alpha n}{\delta} \right)^{-1/\alpha} \left((\alpha + 1) \mathbb{E}_{\frac{\alpha+p-1}{p}} \left(\left(\frac{n\alpha}{\delta} \right)^{-p/\alpha} \lambda^p \right) - \alpha \mathbb{E}_{\frac{\alpha}{p}+1} \left(\left(\frac{n\alpha}{\delta} \right)^{-p/\alpha} \lambda^p \right) \right) \right)$$

$$\begin{aligned}
& + \lambda^{-1} \left(\Gamma\left(\frac{1}{p}\right) - \Gamma\left(\frac{1}{p}, \left(\frac{n\alpha}{\delta}\right)^{-p/\alpha} \lambda^p\right) \right) (p(\alpha+1))^{-1}, \\
\int_0^\infty z^2 M_n(dz) & = \alpha n \left(\left(\frac{\alpha n}{\delta}\right)^{-2/\alpha} \left((\alpha+2) E_{\frac{p+\alpha-2}{p}} \left(\left(\frac{n\alpha}{\delta}\right)^{-\frac{p}{\alpha}} \lambda^p \right) - \alpha E_{\frac{p+\alpha}{p}} \left(\left(\frac{n\alpha}{\delta}\right)^{-\frac{p}{\alpha}} \lambda^p \right) \right) \right. \\
& \left. + 2\lambda^{-2} \left(\Gamma\left(\frac{2}{p}\right) - \Gamma\left(\frac{2}{p}, \left(\frac{n\alpha}{\delta}\right)^{-\frac{p}{\alpha}} \lambda^p\right) \right) \right) (p(\alpha+2))^{-1},
\end{aligned}$$

where $E_m(x) = \int_1^\infty e^{-xt} t^{-m} dt$ is the exponential integral function and $\Gamma(s, x) = \int_x^\infty t^{s-1} e^{-t} dt$ is the upper incomplete gamma function.

Example 2 (continuing from p. 4).

$$\begin{aligned}
\int_{-\infty}^\infty z M_n(dz) & = \delta_+ \left(\left(\frac{\alpha n}{\|\sigma\|}\right)^{-1/\alpha+1} \left((\alpha+1) E_{\frac{\alpha+p-1}{p}} \left(\left(\frac{n\alpha}{\|\sigma\|}\right)^{-p/\alpha} \lambda_+^p \right) - \alpha E_{\frac{\alpha}{p}+1} \left(\left(\frac{n\alpha}{\|\sigma\|}\right)^{-p/\alpha} \lambda_+^p \right) \right) \right. \\
& \left. + \lambda_+^{-1} \frac{\alpha n}{\|\sigma\|} \left(\Gamma\left(\frac{1}{p}\right) - \Gamma\left(\frac{1}{p}, \left(\frac{n\alpha}{\|\sigma\|}\right)^{-p/\alpha} \lambda_+^p\right) \right) \right) (p(\alpha+1))^{-1}, \\
& + \delta_- \left(\left(\frac{\alpha n}{\|\sigma\|}\right)^{-1/\alpha+1} \left((\alpha+1) E_{\frac{\alpha+p-1}{p}} \left(\left(\frac{n\alpha}{\|\sigma\|}\right)^{-p/\alpha} \lambda_-^p \right) - \alpha E_{\frac{\alpha}{p}+1} \left(\left(\frac{n\alpha}{\|\sigma\|}\right)^{-p/\alpha} \lambda_-^p \right) \right) \right. \\
& \left. + \lambda_-^{-1} \frac{\alpha n}{\|\sigma\|} \left(\Gamma\left(\frac{1}{p}\right) - \Gamma\left(\frac{1}{p}, \left(\frac{n\alpha}{\|\sigma\|}\right)^{-p/\alpha} \lambda_-^p\right) \right) \right) (p(\alpha+1))^{-1}, \\
\int_{-\infty}^\infty z^2 M_n(dz) & = \delta_+ \left(\left(\frac{\alpha n}{\|\sigma\|}\right)^{-2/\alpha+1} \left((\alpha+2) E_{\frac{p+\alpha-2}{p}} \left(\left(\frac{n\alpha}{\|\sigma\|}\right)^{-\frac{p}{\alpha}} \lambda_+^p \right) - \alpha E_{\frac{p+\alpha}{p}} \left(\left(\frac{n\alpha}{\|\sigma\|}\right)^{-\frac{p}{\alpha}} \lambda_+^p \right) \right) \right. \\
& \left. + 2\lambda_+^{-2} \frac{\alpha n}{\|\sigma\|} \left(\Gamma\left(\frac{2}{p}\right) - \Gamma\left(\frac{2}{p}, \left(\frac{n\alpha}{\|\sigma\|}\right)^{-\frac{p}{\alpha}} \lambda_+^p\right) \right) \right) (p(\alpha+2))^{-1} \\
& + \delta_- \left(\left(\frac{\alpha n}{\|\sigma\|}\right)^{-2/\alpha+1} \left((\alpha+2) E_{\frac{p+\alpha-2}{p}} \left(\left(\frac{n\alpha}{\|\sigma\|}\right)^{-\frac{p}{\alpha}} \lambda_-^p \right) - \alpha E_{\frac{p+\alpha}{p}} \left(\left(\frac{n\alpha}{\|\sigma\|}\right)^{-\frac{p}{\alpha}} \lambda_-^p \right) \right) \right. \\
& \left. + 2\lambda_-^{-2} \frac{\alpha n}{\|\sigma\|} \left(\Gamma\left(\frac{2}{p}\right) - \Gamma\left(\frac{2}{p}, \left(\frac{n\alpha}{\|\sigma\|}\right)^{-\frac{p}{\alpha}} \lambda_-^p\right) \right) \right) (p(\alpha+2))^{-1},
\end{aligned}$$

where in this case $\|\sigma\| = \delta_+ + \delta_-$.

Example 3 (continuing from p. 4).

$$\begin{aligned}
\int_0^\infty z M_n(dz) &= \left((n\alpha)^{1-\alpha-\beta} \lambda^{\beta/p} \left((\alpha+1)(\alpha+\beta-1)^{-1} {}_2F_1 \left(\frac{\beta}{p}, \frac{\alpha+\beta-1}{p}, \frac{\alpha+\beta+p-1}{p}; -(n\alpha)^{-p}\lambda \right) \right. \right. \\
&\quad + \left. \left((n\alpha)^{\alpha+1} - \alpha - 1 \right) (\alpha+\beta)^{-1} {}_2F_1 \left(\frac{\beta}{p}, \frac{\alpha+\beta}{p}, \frac{\alpha+\beta+p}{p}; -(n\alpha)^{-p}\lambda \right) \right. \\
&\quad \left. \left. - (n\alpha)^{\alpha+1} (\beta-1)^{-1} {}_2F_1 \left(\frac{\beta-1}{p}, \frac{\beta}{p}, \frac{\beta+p-1}{p}; -(n\alpha)^{-p}\lambda \right) \right) \right) \\
&\quad + n\alpha \lambda^{1/p} \Gamma \left(1 + \frac{1}{p} \right) \Gamma \left(\frac{\beta-1}{p} \right) \Gamma \left(\frac{\beta}{p} \right)^{-1} (\alpha+1)^{-1},
\end{aligned}$$

if $\alpha + \beta > 1$ and $\beta \neq 1$, where ${}_2F_1(a, b, c; x) = \sum_{j=0}^{\infty} \frac{(a)_j (b)_j}{(c)_j} \frac{x^j}{j!}$ is the hypergeometric function and $(q)_j$ denotes the Pochhammer symbol. We omit the formula for $\beta = 1$.

$$\begin{aligned}
\int_0^\infty z^2 M_n(dz) &= \left((n\alpha)^{2-\alpha-\beta} \lambda^{\beta/p} \left((\alpha+2)(\alpha+\beta-2)^{-1} {}_2F_1 \left(\frac{\beta}{p}, \frac{\alpha+\beta-2}{p}, \frac{\alpha+\beta+p-2}{p}; -(n\alpha)^{-p}\lambda \right) \right. \right. \\
&\quad + \left. \left(2(n\alpha)^{\alpha+1} - \alpha - 2 \right) (\alpha+\beta)^{-1} {}_2F_1 \left(\frac{\beta}{p}, \frac{\alpha+\beta}{p}, \frac{\alpha+\beta+p}{p}; -(n\alpha)^{-p}\lambda \right) \right. \\
&\quad \left. \left. - 2(n\alpha)^{\alpha+1} (\beta-2)^{-1} {}_2F_1 \left(\frac{\beta-2}{p}, \frac{\beta}{p}, \frac{\beta+p-2}{p}; -(n\alpha)^{-p}\lambda \right) \right) \right) \\
&\quad + n\alpha \lambda^{2/p} \Gamma \left(1 + \frac{2}{p} \right) \Gamma \left(\frac{\beta-2}{p} \right) \Gamma \left(\frac{\beta}{p} \right)^{-1} (\alpha+2)^{-1},
\end{aligned}$$

if $\alpha + \beta > 2$ and $\beta \neq 2$. We omit the formula for $\beta = 2$.